Parametric active contour and directed balloon energy Tracking textured objects against textured backgrounds using the Walsh-Hadamard transform.

Dr. AVULA MAHESWARA RAO [1],S MUNIRAJA [2]

Abstract :*Active contour models (ACM) are a well-liked method for identifying and following object boundaries. Using a new balloon energy in parametric active contour, this article demonstrates how to follow a texture item against a texture backdrop. This suggested technique elaborates on the energy function of the parametric ACM by include the balloon energy to enable accurate identification and tracking of texture targets against texture backgrounds. This technique uses a variant of the Walsh-Hadamard transform called the direc tional Walsh-Hadamard transform to compute the texture features of contour and object points. The balloon's movement direction is next calculated by comparing the texture feature of contour points to the texture feature of the target object; finally, the contour curves are either enlarged or reduced such that they fit inside the confines of the target. The procedure of tracking is repeated till the very final frames. When compared to the moment-based active contour technique, our approach is superior at tracking object boundary edges in video streams with dynamic backgrounds. Due to its lesser complexity, our solution not only improves tracking accuracy but also converges faster.*

Introduction

Many computer vision applications, including traffic monitoring in ICT systems, video surveillance, medical applications, military object tracking, object-based video compression, etc. [1-4], find object tracking to be one of the most intriguing issues. Tracking refers to the process of detecting and comparing the motion of an item throughout a series of still images or moving video. A wide range of tracking approaches, from the straightforward and rigid object tracking with a stationary camera to the more complicated and non-rigid object tracking with a moving camera, have been suggested and refined [5]. These techniques may be broken down into the following five classes: region-based [6,7], feature-based [8,8], mesh-based [10,11], model-based [12,13], and active contour models (ACM)-based [6,8]. Kass first proposed the active contour approach in 1987 [14]. The two primary categories of ACM are parametric and geometric active contours. Two- or three-dimensional pictures begin with a parametric ACM curve. Both internal and external influences shape it, and it ceases at the image's actual edges. Segmentation and video object tracking using this technique was presented; nevertheless, it has a number of drawbacks, including slowness and lack of precision [15]. The idea of curve evolution and level set procedures underpin the geometric ACM

proposed by Caselless and Malladi [16,17], whereby curves and levels are ranked according to certain geometric criteria. One of the many benefits is that it can identify the borders of many objects at once. Geometric active contour, however, is slower than parametric ACM because of its. Higher computing cost and complexity. However, conventional parametric ACM fails to accurately identify object boundaries when there are no prominent edges present. Both Ivins and Por rill [18] and Schaub and Smith [19] presented alternative color active contours as a solution to this issue. Their technique involves pointing contour curves in the direction of a coloured target item. With this strategy, even targets with blurry edges may be located and followed. The most glaring drawback is that the approach cannot track objects with complex color or texture, hence the object and backdrop color must be basic.

Assistant professor1,2
DEPARTMENT OF ELECTRONICS AND COMMUNICATION ENGINEERING
P.B.R.VISVODAYA INSTITUTE OF TECHNOLOGY & SCIENCE
S.P.S.R NELLORE DIST, A.P , INDIA , KAVALI-524201

ACM as described by mathematics as described in [14], a snake is a kind of parametric curve used in parametric ACM.

$$S(u) = I(x(u), y(u)), u \in [01]$$

I is the image intensity at (x,y). In order to implement, the vector function S(u) is approximated discontinuously at $\{ui\}$, i = 0, 1,..., M, in which M is the number of points on the contour. Finally, continuous curve will be obtained from interpolation of these points. The traditional flexible parametric method is based on the application of contour, which minimizes the weighted sum of the internal and external energies. Therefore, the final contour is defined by minimizing the following energy function.

$$E(s(u)) = E_{int}(s(u)) + E_{img}(s(u)),$$

where Eint is the internal energy of the contour defined as follows: Eint

$$E_{int} = \frac{\alpha}{2}\left|\frac{\partial}{\partial u}S(u)\right|^2 + \frac{\beta}{2}\left|\frac{\partial^2}{\partial u^2}S(u)\right|^2$$

In the above equation, the first and second parts of the energy equation prevent contour from excessive stretching and bending along with preserving its coherence and smoothness. Weighting parameters, α and β, are used to adjust the properties of elasticity and rigidity. Image energy directs contour curve to desirable features such as edges, lines, and corners. This energy in initial formula of ACM is defined and approximated to detect the edge and is calculated as [22]

$$E_{img} = E_{edge} = -P\left|\nabla(G_\sigma(s) * I(s))\right|^2$$

$$m_{01} = \begin{bmatrix} -1 & 0 & 1 \\ -1 & 0 & 1 \\ -1 & 0 & 1 \end{bmatrix} \quad m_{10} = \begin{bmatrix} -1 & -1 & -1 \\ 0 & 0 & 0 \\ 1 & 1 & 1 \end{bmatrix} \quad m_{00} = \begin{bmatrix} 1 & 1 & 1 \\ 1 & 1 & 1 \\ 1 & 1 & 1 \end{bmatrix}$$

$$m_{11} = \begin{bmatrix} 1 & 0 & 1 \\ 1 & 0 & 1 \\ 1 & 0 & 1 \end{bmatrix} \quad m_{02} = \begin{bmatrix} 1 & 0 & -1 \\ 0 & 0 & 0 \\ -1 & 0 & 1 \end{bmatrix} \quad m_{20} = \begin{bmatrix} 1 & 1 & 1 \\ 0 & 0 & 0 \\ 1 & 1 & 1 \end{bmatrix}$$

Figure 1 The masks corresponding to the moment up to order two with window size of 3 × 3 [15]

where Gσ is a 2D Gaussian kernel with standard deviation σ, ∇ and * present gradient and convolution operators, respectively. P is the weighting parameter that controls the image energy which is constant. Equation (4) is used for noise reduction by applying a Gaussian filtering. Consequently, the total energy of active contour is defind as follows

$$E = \frac{\alpha}{2}\oint\left|\frac{\partial}{\partial u}S(u)\right|^2 du + \frac{\beta}{2}\oint\left|\frac{\partial^2}{\partial u^2}S(u)\right|^2 du + \oint E_{edge}(S(u))du$$

We suggest using the pressure energy of textures to detect and follow texture objects against a texture backdrop. In the ACM energy function [15], this pressure energy takes the role of the edge energy. Then, a moment-based approach has been used to extract texture characteristics. Six masks of size 33 are shown in Figure 1 to represent the moments up to order 2.

Strategy Advised

Here, we will first break out how DWHT extracts features. Then, in Section 4.2, we provide the balloon energy that is based on DWHT. The suggested approach is then used to show a tracking algorithm in Section 4.3. In Section 4.4, we discuss the criteria for terminating the contour.

The DWHT Method for Extracting Features

Following is the DWHT feature extraction process. First, you'll need to calculate a 4x4 local window (A) centered on the object and contour points. Rotating A by angles of = 0°, 45°, 90°, 135° produces the four corresponding matrices A0°, A45°, A90°, and A135°. Third, we get the sequence bands b1, b2, and b3 by dividing each matrix in 2 by 1 4 ; 1 4 ; 1 2 (see Equation 15). F(i, j)=[F1,..., F12] is the formula used to get the mean of each band and is the texture feature vector. Figure 3 is a block diagram depicting this process.

DWHT-powered balloons

Cohen first proposed the concept of balloon energy in 1991 [29]. Balloon energy is used for DWHT computed texture characteristics in this research. Using Equation (4), we can determine that the external energy is equal to 14 Eimg Ebal 16 ESCB. The normal unitary vector (n s) and the threshold

function (B) are both described as BIs, therefore the texture-based energy (ESCB) is written as Ebal 14 BIS n s 17.

$$E_{ext} = E_{img} + E_{bal}$$

ESCB is obtained by Equation (4). ESCB as a texture-based energy is defined a

$$E_{bal} = B(I(S)) \times \vec{n}(s)$$

where $\vec{n}$ sð Þis the normal unitary vector and B is a threshold function which is defined

$$B(I(s)) = \begin{cases} 1 & \text{if } \dfrac{F(I(s)) - O\mu}{O_\sigma} < K \\ -1 & \text{otherwise} \end{cases}$$

where F is the texture feature vector of contour, and Oμ and Oσ are the mean and standard deviation of the F_ob vector, respectively, F_ob is the texture feature vector of the target object points (see Figure 3). K is defined as follows

$$k_i = 2 \times \frac{|B\mu_i - O\mu_i|}{O\sigma_i}$$

where $\beta\mu$ is the mean of feature vector of background. By calculating Equation (19), 12 K parameters are achieved, then variance and maximum of K vector are calculated, after that, the distance between them is obtained. Each of the K parameters which is bigger than this number will be selected. K parameters which have the above-mentioned features are used in Equation (18). It is evident that compared with [20] the K parameters are obtained automatically.
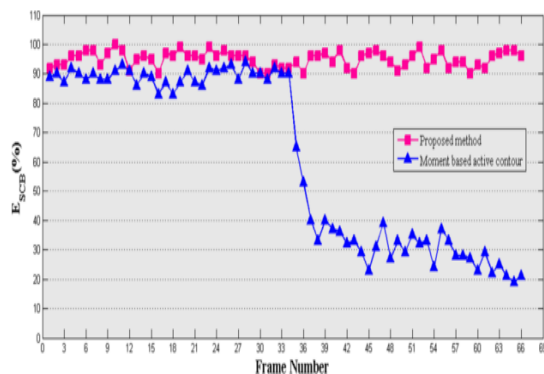

Figure 2 Comparative diagram of ESCB for two methods calculated for each frame

Balloon force allows the contour curve to expand or to shrink in order to fit to the target boundaries. Consequently, the new energy of active contour is

$$E = \underbrace{\frac{\alpha}{2}\oint\left|\frac{\partial}{\partial u}S(u)\right|^2 du + \frac{\beta}{2}\oint\left|\frac{\partial^2}{\partial u^2}S(u)\right|^2 du}_{\text{Internal Energy}} + \underbrace{\oint E_{ext}(S(u))du}_{\text{External energy}}$$

The result of the experiments

In this section, we have implemented the proposed method (balloon energy based on DWHT added to parametric active contour) and a moment-based active contour method in MATLAB and the results are compared in terms of speed and accuracy. In this article, we have tried to make the images more realistic than [20] by preparing different texture environments and then capturing films from those environments. In this way at least the filming process is done realistically. All experiments are performed using2.5 GHz Intel Core 2 Dou processor with windows Vista. In these
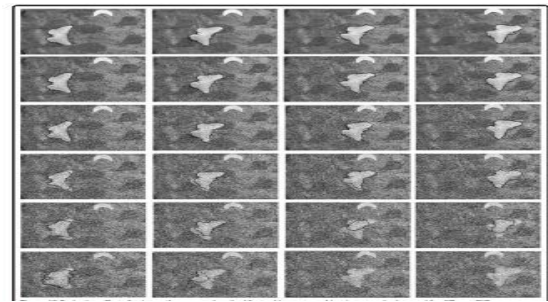

Figure 3 Evaluating effect of noise on the proposed method for tracking texture object in texture background for different SNR. SNR = 14.47 dB (1strow), 7.48 dB (2ndrow), 4.47 dB (3rdrow), 2.70 dB (4throw), 1.46 dB (5throw), and 0.49 dB (6throw) for frames from left to right:1, 20, 30,41.

experiments, different texture objects in various texture backgrounds were used.The frame size is chosen to be 352 × 288 pixels. Figure 6 shows the tracking result of the proposed method and moment-based active contour of the first experiment. In this experiment, background is made of two different cloth's materials, satin and silk. As Figure 6A shows, the moment-based active contour cannot detect the object boundary correctly. On the other hand, regarding to the moment-based active
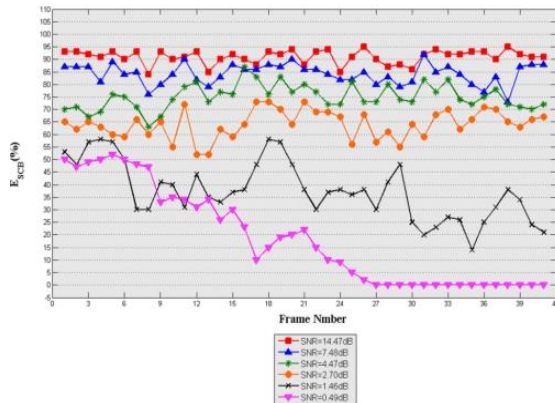
figure 4 ESCB diagram of the proposed method for the sequence including 41 frames in different value of SNR.

contour proposed method could detect and track object boundaries in all frames with high accuracy (Figure 4B). Figure 4 shows the place of initializing the snake and its evolution in different iteration until the snake is adapted in object boundary for the first frame. The number of iterations is automatically adjusted, which results in decreasing of tracking time

To measure the accuracy of tracking, we employed the error criterion introduced in [30]:

ESCB ¼ SCB nð Þ n ð22Þ where n is the obtained number of contour points, SCB(n) refers to the number of contour points on the correct boundary. This measure converges to 100% when the correct boundary detection is achieved. Figure 8 shows

table 2 The average of ESCB for different values of SNR

	SNR (dB)					
	14.47	7.48	4.47	2.70	1.46	0.49
Average of E_{SCB} (%)	91.27	84.18	75	64.07	37.49	18.83

comparative diagram of ESCB for these two methods. Table 1 demonstrates the average of ESCB and the convergence speed of two methods for 41 frames. In the second experiment (Figure 9), the performance of proposed method is compared with moment-based active contour when the texture of background is changed. This experiment is designed in such a way that a texture object moved from a texture background to another one. The former texture is made from fabric and the latter is a wooden texture. Relevant figures are shown in Figure 9. As shown in Figure 9A, the moment-based active contour cannot be detected and the object boundary in the frames in background transition occurs. The contour is expanded in these frames. Then, since these false contours will be the initial contours of

next frames, the error would be propagated and the contour would not fit to edges any more. But regarding to the moment-based active contour, our proposed method is successful in detecting object boundary and correctly tracking target objects in all frames despite the changes of texture background (Figure 9B). Figure 10 shows the place of initializing the snake and its evolution in different iteration until the snake is adapted in object boundary for the first frame
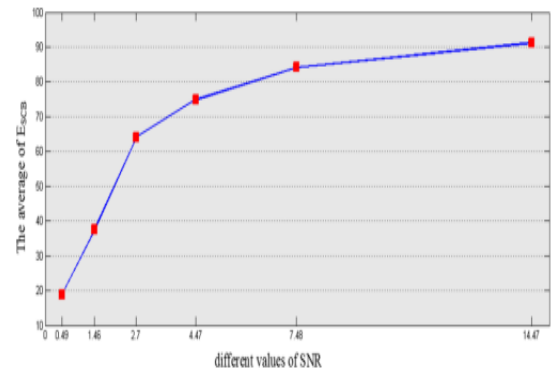

figure 5The average of the ESCBfor different SNR values

The ESCB comparison diagram between the two approaches is shown in Figure 5. The average ESCB and convergence speed of two approaches over 50 frames are shown in Table 1. When the toy bus travels in front of the teddy bear, we tested the effectiveness of the suggested and moment-based active contour approaches in a third experiment shown in Figure 15. When the toy bus moved in front of the teddy bear, the moment-based active contour was unable to identify the target item because the contour curve was stretched. However, the suggested approach is still able to detect the toy bus more accurately than the moment-based active contour. Figure 13 shows where the snake is initially initialized and how it changes over time to fit inside the object boundary in the first frame. Once again, the experiment results demonstrate the improved performance of the suggested strategy. The ESCB comparison diagram between the two approaches is shown in Figure 5. Average ESCB and convergence speed for two approaches across 66 frames are shown in Table 1. The suggested approach is 33% more accurate than the moment method, and the DWHT has a 74.18% faster convergence rate.

Conclusion

Moment-based parametric active contours were developed for texturing object tracking. The model fails to accurately identify the target item when the texture backdrop is dynamic. In such instances, the target's contour curve is widened. In this piece, we extend parametric active contour with a balloon energy that takes texture into account. The DWHT calculation used to determine the texture feature is

dependent on the direction of the balloon. The experimental findings show that our technique outperforms the moment-based method in terms of tracking accuracy. More so than moment-based active contour, DWHT has a faster convergence rate. We test the method's robustness against varying amounts of Gaussian noise. The results demonstrate the suggested approach is very noise-tolerant. As a consequence, tracking the target item is successful even when the backdrop is textured. As a result, objects against textured backgrounds may be identified more accurately.

References

[1]. H Eng, M Thida, B Chew, K Leman, S Anggrelly, Model-based detection and segmentation of vehicles for intelligent transportation system, in 3rd IEEE Conference on Industrial Electronics and Applications, (Singapore, 2008), pp. 2127–2132

[2]. K Huang, T Tan, Vs-star: A visual interpretation system for visual surveillance. Pattern Recognit. Lett. 31(14), 2265–2285 (2010)

[3]. N Sirakov, H Kojouharov, N Sirakova, Tracking neutrophil cells by active contours with coherence and boundary improvement filter, in Image Analysis & Interpretation (SSIAI), (Austin, TX, USA, 2010), pp. 5–8

[4]. M Lee, W Chen, C Lin, C Gu, T Markoc, S Zabinsky, R Szeliski, A layered video object coding system using sprite and affine motion model. IEEE Trans. Circuits Syst. Video Technol. 7(1), 130–145 (1997)

[5]. Q Sun, P Heng, D Xia, Two-stage object tracking method based on kernel and active contour. IEEE Trans. Circuits Syst. Video Technol. 20(4), 605–609 (2010)

[6]. K Hariharakrishnan, D Schonfeld, Fast object tracking using adaptive block matching. IEEE Trans. Multimed. 7(5), 853–859 (2005)

[7]. A Cavallaro, From visual information to knowledge: semantic video object segmentation, tracking and description, PhD thesis (EPFL Switzerland, 2002)

[8]. P Salembier, F Marqúes, Region-based representations of image and video: segmentation tools for multimedia services. IEEE Trans. Circuit Syst. Video Technol. 9(8), 1147–1167 (1999)

[9]. P Moallm, A Memmarmoghaddam, M Ashourian, Robust and fast tracking algorithm in video sequences by adaptive window sizing using a novel analysis on spatiotemporal gradient powers. Int. J. Circuit Syst. Comput. 16(2), 305–317 (2007)

[10]. I Celasun, A Tekalp, Optimal 2-D hierarchical content-based mesh design and update for object-based video. IEEE Trans. Circuit Syst. Video Technol. 10(7), 1135–1153 (2000)

[11]. A Dufour, R Thibeaux, E Labruyère, N Guillén, J Olivo-Marin, 3-D active meshes: fast discrete deformable models for cell tracking in 3-D time-lapse microscopy. IEEE Trans. Image Process 20(7), 1925–1937 (2011)

[12]. A Comport, E Marchand, F Chaumette, Efficient model-based tracking for robot vision. Adv. Robot. 19(10), 1097–1113 (2005)

[13]. X. Bing, Y. Wei, C. Charocnsak, Face contour tracking in video using active contour model, in Proceedings of the IEEE International Conference on Image Processing., vol. 2 (Singapore, 2005), pp. 1021–1024

[14]. M. Kass, A. Witkin, D. Terzopoulos, Snakes: active contour models. International Journal of Computer Vision, London 1(4), 321–331 (1987)

[15]. A Vard, P Moallem, A Naghsh, Texture based parametric active contour target detection and tracking. Int. J. Imag. Syst. Technol. Wiley 19(3), 187–198 (2009)

[16]. V Caselles, F Catte, T Coll, A geometric model for active contours, in International Conference on Image Processing., vol. 66 (Washington, DC, 1995), pp. 1–31

[17]. R Malladi, J Sethian, B Vemuri, Shape modeling with front propagation: a level set approach. IEEE Trans. Pattern Anal. Mach. Intell. 17(2), 158–175 (1995)

[18]. J Ivins, J Porrill, Active region models for segmenting medical images, in Proceedings of the 1st international conference on image processing. vol. 2 (Austin TX, USA, 1994), pp. 227–231.

[19]. H Schaub, C Smith, Color snakes for dynamic lighting conditions on mobile manipulation platforms, in Proceedings of the IEEE/RSJ international conference on intelligent robots and systems. vol. 2 (Albuquerque, NM, USA, 2003), pp. 1272–1277.

[20]. A Vard, A Monadjemi, K Jamshidi, N Movahhedinian, Fast texture energy based image segmentation using directional Walsh–Hadamard transform and parametric active contour models. Expert Syst. Appl. 38(9), 11722–11729 (2011)

[21]. A Monadjemi, P Moallem, Texture classification using a novel Walsh/ Hadamard transform, in 10th WSEAS International Conference on Computers (Athens, Greece, 2006), pp. 1055–1060.